Hydrogen for Long-duration Energy Storage in a Fully Renewable Island Power System: A Case Study of Reunion Island

Mirabelle Scholten[1], Agnès François[2], Robin Roche[1], Dominique Grondin[3], and Halima Ikaouassen[1]
[1]*Université Marie et Louis Pasteur, UTBM, CNRS, institut FEMTO-ST*, F-90000 Belfort, France
{mirabelle.scholten, robin.roche, halima.ikaouassen}@femto-st.fr
[2]*CEA, CEA Tech Occitanie*, F-31670 Labège, France
agnes.francois@cea.fr
[3]*ENERGY-lab, Université de La Réunion*, Saint-Denis, France
dominique.grondin@univ-reunion.fr

***Abstract*—The transition to fully renewable energy systems poses unique challenges for non-interconnected islands due to the intermittency of renewable generation, limited land availability, and lack of grid interconnections, making long-duration energy storage essential. This paper presents a multi-objective optimization approach to assess the techno-economic and environmental viability of hydrogen energy storage (HES) in future fully renewable island power systems. Using Reunion Island as a case study with three five-year weather periods, results indicate HES is critical during extended low-solar events, though infrequently used. The analysis highlights significant impacts of weather-year selection on optimal HES capacity, underscoring the importance of accounting for climatic variability in island energy planning.**

***Index Terms*—Hydrogen, Long-duration energy storage, Multi-objective optimization, Reunion Island, Renewable energy**

I. Introduction

As climate change impacts intensify, the shift to fully renewable energy systems has become essential. For non-interconnected islands, however, the intermittency of renewables, limited network capacities, and network isolation threaten demand fulfillment [1]. Energy storage offers a key solution to these challenges.

Batteries are the most widely used storage technology in both island [2] and non-island [3] systems, providing mature, cost-effective short-duration storage from seconds to several hours [4]. Hydrogen, by contrast, is an emerging option for long-term storage, capable of spanning days to seasons with minimal self-discharge [5]. These features make hydrogen energy storage (HES) especially relevant for non-interconnected grids, where balancing supply and demand over longer horizons is crucial [6].

Several studies have compared batteries, hydrogen, and hybrid configurations in island systems from technical, economic, and environmental perspectives [7]–[10]. Their findings indicate that the optimal role of HES depends largely on the match between local weather and demand profiles. Moreover, as noted in [11], evaluating both economic and environmental costs is necessary to assess HES viability. This highlights the need for multi-objective optimization to determine whether, and at what scale, HES is feasible under island conditions.

This paper presents a methodology for assessing the economic and environmental performance of HES in future fully renewable systems, demonstrated through a case study of Reunion Island. To date, no studies have examined the potential scale of HES deployment there, despite its target of achieving full renewable self-sufficiency by 2030 [12]. Section II details the optimization framework, Section III introduces the case study, Section IV discusses key findings on HES operation relative to renewable generation, and Section V summarizes contributions and future work. This study forms part of the doctoral thesis in [13].

II. Methodology

This section presents the methodology used to assess the technical feasibility and environmental-economic optimality of hydrogen energy storage (HES) in a fully renewable island power system. The approach combines a detailed power system model with a multi-objective optimization (MOO) framework that jointly minimizes total system costs and lifecycle greenhouse gas emissions. The following subsections describe the storage technology modeling, optimization formulation, objective functions, and constraints in detail, after which a summary figure of the overall workflow is provided. This work uses Python for Power System Analysis (PyPSA) to model the transmission network and storage technologies, with Gurobi as the optimization solver.

A. Energy Storage Model

This study considers batteries and hydrogen as plausible energy storage technologies, assumed to be deployable at any transmission substation. Despite many different available battery chemistries, this study only considers Lithium-iron-phosphate due to its suitability for stationary use [14]. These two storage types were selected for their complementary characteristics: batteries are a mature technology that offers high round-trip efficiency and fast response times for short-term balancing, while above-ground, low-pressure HES provides a developing solution for long-duration energy storage with limited geographical limitations. Although other storage technologies may be applicable, this focused selection captures the key storage dynamics in high-renewable systems while keeping the model tractable to demonstrate the methodology's functionality.

The operation of a battery within the PyPSA model is described by (1), (2), and (3) adapted from [15]. In (1), the power, P_B, in (i) or out (o) of the battery is constrained by the rated power of the battery $\bar{P}_B$. The subscript B denotes that these values are for a battery, $n \rightarrow \{1, ..., N\}$ is used to represent each substation of the transmission network model, while the subscript $t \rightarrow \{1, ..., T\}$ is used to refer to each hour of the simulated time horizon.

$$-\bar{P}_{B,n,t} \leq P_{B,i/o,n,t} \leq \bar{P}_{B,n,t} \tag{1}$$

Additionally, the energy stored in each battery in the network at any moment in time, $E_{B,n,t}$, is limited to be between 15% of the rated capacity and the rated capacity, $\bar{E}_{B,n}$ as shown in (2).

$$0.15 \cdot \bar{E}_{B,n} \leq E_{B,n,t} \leq \bar{E}_{B,n} \tag{2}$$

Finally, between each time step, the evolution of the state of charge of each battery is described by (3). Furthermore, η_{auto} represents the auto-discharge of the battery, and $\eta_{B,i}$ is the battery's charge efficiency. It should be noted that the discharge efficiency of the battery is considered in the model's energy balance shown in (11).

$$E_{B,n,t} = \eta_{auto} \cdot E_{B,n,t-1} + P_{B,i,n,t} \cdot \eta_{B,i} \cdot \Delta t - P_{B,o,n,t} \cdot \Delta t \tag{3}$$

HES uses an electrolyzer to convert excess power to hydrogen, stored at 30 bars in above-ground tanks. Alternative storage methods are not considered due to site-specific requirements, energy penalties, and limited commercial deployment [16]. Finally, a fuel cell is used to convert hydrogen back to electrical power. Fuel cells are chosen over internal combustion engines (ICEs) due to higher efficiency, lower maintenance, and reduced emissions [17].

The operation of the HES is dictated by a modified, mass-based versions of (3), (2), and (1), presented in equation (4), (5), (6), respectively. In these equations, the HES tank operation is managed in terms of mass, m and the rated storage mass, $\bar{m}$, in kilograms, and the mass flow rate, $\dot{m}$, and the rated mass flow rate, $\bar{\dot{m}}$, in kilograms per hour. Additionally, there is negligible auto-discharge [18], and the charge efficiency is assumed to be 100% with conversion efficiencies from the fuel cells and electrolyzers accounted for in equations (11) and (12).

$$m_{H_2,n,t} = m_{H_2,n,t-1} + \dot{m}_{H_2,i,n,t} \cdot \Delta t - \dot{m}_{H_2,o,n,t} \cdot \Delta t \tag{4}$$

$$0 \leq m_{H_2,n,t} \leq \bar{m}_{H_2,n} \tag{5}$$

$$-\bar{\dot{m}}_{H_2,n,t} \leq \dot{m}_{H_2,i/o,n,t} \leq \bar{\dot{m}}_{H_2,n,t} \tag{6}$$

Finally, an additional constraint of cyclical operation over the time horizon, T is implemented with a tolerance of 10% to ensure the storage system returns to approximately the same starting state at the time horizon's end to allow for operational continuity beyond the modeled time horizon. This is described by (7) where t_0 is the initial hour of the time horizon T and t_f is the final hour.

$$m_{H_2,n,t_0} \cdot (1-10\%) \leq m_{H_2,n,t_f} \leq m_{H_2,n,t_0} \cdot (1+10\%) \tag{7}$$

B. Optimization Model

A significant consideration with regard to modeling long-duration energy storage is the length of the time horizon that is modeled and optimized. While single-year models account for seasonal variations, they miss inter-annual variations in weather and demand patterns where long-duration storage such as hydrogen could provide value [19]–[21]. However, the choice regarding how many years to model ultimately depends on data availability and computational tractability.

Within the model, each substation can install a hydrogen and a battery energy storage system. As such, the optimization variables of this model are as follows:

- Fuel cell power ratings and hourly power dispatch in MW
- Electrolyzer power ratings and hourly power dispatch in MW
- Each H_2 gas storage tank's capacity and hourly state of charge in MWh
- The hourly in- and outlet flow rates of each H_2 gas storage tank in kg H_2
- Battery capacity and hourly state of charge at each substation in MWh
- The hourly in- and outlet power of each battery in MW
- The hourly electricity mix in MWh
- The power network's line capacities in MVA

The objective function for the minimization of the investment and operating costs is that presented in (8) which was adapted from [15] and where C_s represents the investment costs of component type s and O_s represents the operating costs.

$$\begin{aligned}\min \sum_{n} & [C_{FC}(\bar{P}_{FC,n}) + C_{ely}(\bar{P}_{ely,n}) \\ & + C_{H_2}(\bar{E}_{H_2,n}) + C_B(\bar{E}_{B,n})] \\ & + \sum_{n,t} [O_{ely}(E_{ely,n,t}, C_{ely}) + O_{H_2}(C_{H_2,n})] \\ & + \sum_{n,t} [O_B(E_{B,n,t}, \bar{E}_{B,n})] + \sum_{l} C_l\end{aligned} \tag{8}$$

Here, C_l represents the investment cost associated with an increase in the capacity in each transmission line l and is described by (9) from [22], where p_c^{new} is the price of the conductor per kilometer at the new line capacity, p_f is the fixed cost associated with the replacement of the conductor, L_l is the line length and 1.2 is a factor to account for extra costs due to the island context.

$$C_l = 1.2 \cdot (p_c^{new} + p_f) \cdot L_l \tag{9}$$

The environmental objective function, shown in (10), minimizes the total Global Warming Potential (GWP) of the storage solutions, where Env_s represents the total GWP of each component type. GWP is a single metric that accounts for the warming impact of a technology's greenhouse gas emissions throughout its entire lifecycle, including raw material extraction, production, transportation, usage, recycling, and end-of-life. It is expressed in kilograms of CO_2 equivalent emissions. Grid operation is assumed to contribute minimal lifecycle GWP emissions because the system is fully renewable and relies on locally sourced biomass.

$$\min \sum_{n} [Env_B \cdot \bar{E}_{B,n} + Env_{H_2} \cdot \bar{E}_{H_2,n} + Env_{FC} \cdot \bar{P}_{FC,n} + Env_{ely} \cdot \bar{P}_{ely,n}] \tag{10}$$

To implement the multi-objective optimization, the ϵ-constraint method was implemented, allowing one objective to be optimized while treating other as a constraint.

The optimization is also technically constrained. Firstly, at every time step, the electrical power must be balanced within the system, as described by (11) modified from [15]. In this equation, G refers to the power generated by technology s at timestep t and substation n. $P_{FC,n,t}$ is the power produced by the fuel cell and η_{FC} is the efficiency of conversion between hydrogen to electricity of the fuel cell. η_o is the discharge efficiency of the battery. Also, $f_{l,t}$ represents the power flowing through line l where $l \to \{1, ..., L\}$ is used to represent each line of the transmission network model, and K_{nl} is the incidence matrix of the transmission network. $D_{n,t}$ is the hourly power demand at each substation,n.

$$\begin{aligned} &\sum_{s} G_{n,s,t} + \sum_{n} P_{FC,n,t} \cdot \eta_{FC} - \sum_{n} P_{B,i,n,t} \\ &+ \sum_{n} P_{B,o,n,t} \cdot \eta_{B,o} - \sum_{l} K_{nl} \cdot f_{l,t} = \sum_{n} D_{n,t} \\ &+ \sum_{n} P_{ely,n,t} \end{aligned} \tag{11}$$

Similarly, the hydrogen balance, as described by (12), must be respected at each time-step, where η_{ely} is the energy consumption of the electrolyzer per kilogram of hydrogen. Additionally, $m_{FC,n,t}$ represents the mass quantity of hydrogen consumed by the fuel cell at substation n of the network at time step t.

$$\sum_{n} \frac{P_{ely,n,t}}{\eta_{ely}} = \dot{m}_{H_2,i,n,t} - \dot{m}_{H_2,o,n,t} + \dot{m}_{FC,n,t} \tag{12}$$

Additionally, the power produced by the different renewable energy sources is constrained by a maximum and minimum p.u. restriction, $\underset{\vee}{G}_{n,s,t}$ and $\hat{G}_{n,s,t}$ as shown in (13) sourced from [15], where $\overset{\vee}{\bar{G}}_{n,s}$ is the nominal power of generator type s.

$$\underset{\vee}{G}_{n,s,t} \cdot \bar{G}_{n,s} \leq G_{n,s,t} \leq \hat{G}_{n,s,t} \cdot \bar{G}_{n,s} \tag{13}$$

Finally, the power traveling over each line in the transmission network is limited by the capacity of the line, F_l, which is in turn constrained in the optimization by the maximum possible line capacity, $\hat{F}_l$ as described in (14) from [15].

$$|f_{l,t}| \leq F_l \leq \hat{F}_l \tag{14}$$

To summarize the modeling and optimization process, figure 1 visually outlines the methodology presented in this section. It consolidates the model inputs which include the island network, generation and storage data, objectives, and constraints, and shows the resulting outputs, including the Pareto front of optimal storage configurations and the charge–discharge profiles.

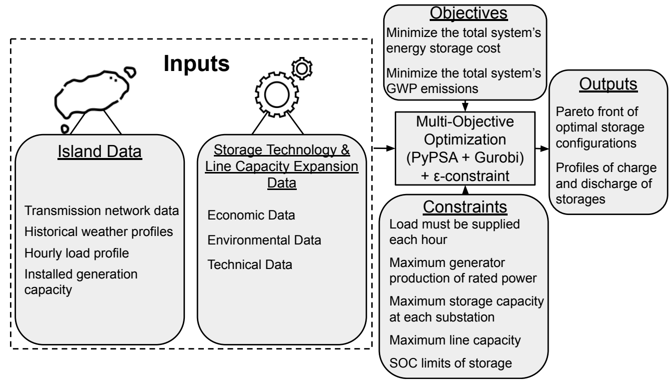

Fig. 1. Methodology of the multi-objective optimization of energy storage for a fully renewable island power system

III. Reunion Island

Reunion Island, a French department in the south Indian Ocean with over 880,000 people [23] with about 43% protected land [24]. In 2023, 56.6% of the island's electricity was produced by renewable sources, mainly from different forms of biomass and hydroelectric production, but 88.6% of the island's energy was imported [25]. The island targets complete renewable self-sufficiency by 2030 [12], with studies identifying energy storage as essential to make this happen [13], [26], [27].

To apply the methodology defined in section II, information regarding Reunion Island's grid, electricity supply and demand, and techno-economic and environmental data regarding the storage technologies is needed and summarized in the following subsections.

A. Grid Network Model

In terms of the power system on Reunion Island, [27] already developed a transmission network model in PyPSA, which includes the 520 km of 63kV transmission lines along with 26 transmission substations using open source data from [28]. Line capacities were assumed to be 44.7 MVA and 26.2 MVA for parallel lines, with maximum extendable capacity of 88 MVA [22] and associated upgrade costs presented in Table I.

B. Electricity Generation

The installed capacities of the power generation technologies considered in this work are presented in Table II.

TABLE I
Line capacity upgrade costs

Cost Parameter	Value	Unit
$p_c^{39\ \mathrm{MVA}}$	4.9	k€/km
$p_c^{50\ \mathrm{MVA}}$	7.4	k€/km
$p_c^{67\ \mathrm{MVA}}$	10.4	k€/km
$p_c^{88\ \mathrm{MVA}}$	14.9	k€/km
p_f	25	€/km

These capacities originate from a scenario referred to as 2050 combined from a previous work of [27], where a fully renewable energy target was set for 2050 and Ocean Thermal Energy Conversion (OTEC) and geothermal sources were considered for base power generation, while local Photovoltaic (PV), hydropower, and biomass resources are exploited to their maximum potential. In the developed PyPSA model, power production and consumption are assessed on an hourly resolution for the assessed time horizon, T. Historical hourly weather data (2000–2015) from 15 Météo France stations were used to assess the power generation from the installed capacities. To balance computational tractability and capture inter-annual variability, the 15 years were divided into three five-year periods.

TABLE II
INSTALLED GENERATION CAPACITY IN 2050

Technology	Installed Capacity (MW)
Onshore Wind	146.05
Offshore Wind	40.00
Geothermal	15.00
PV	1222.69
Hydropower	238.17
OTEC	31.00
Biomass	320.30

C. Electricity Demand

With regard to power systems modeling, besides generation, consumption data is a key input parameter in order to ensure demand is met at all times and thus the system is reliable. For Reunion Island, no hourly consumption data is publicly available at a substation resolution. So, EDF Opendata [28] for 2019 hourly production was used to create synthetic demand profiles for each substation via a probabilistic bottom-up modeling method presented in [13]. Due to the high uncertainty of future electricity demand, the energy efficiency scenario from a French Agency for Ecological Transition (ADEME) report was adopted, which projects a medium-term slowdown and complete vehicle electrification with an 80% controllable fleet by 2050 [29], [30].

D. Technical, Economic and Environmental Data for Storage Technologies

The key economic and environmental parameters of the two storage technologies considered are summarized in Table III, where CAPEX is the capital expenditure and O&M is the operating and maintenance. The environmental impact of the storage technologies considered in this study is presented in terms of their GWP in tables IV and V. Table V presents an estimation of the GWP resulting from the transportation of the components to Reunion Island, calculated using the methodology developed in [31]. It is assumed that all originate from mainland France.

IV. RESULTS

The state of charge evolution of the sum of the hydrogen and battery storage systems for the optimization periods of 2000 through 2004, 2005 through 2009, and 2010 through 2014 is shown in figure 2 (a)-(c). In general, the figures show a highly intermittent use of the stored energy in the form of hydrogen, reserved for use only a few times over the five-year periods. For each time horizon, the initial state of charge of the HES is approximately that of the final state of charge, aligning with the constraint imposed by (7). However, it can be seen that there is a great difference in the starting states of the HES between the periods. Fig. 2 (a) requires 0.19 GWh of initial HES charge while Fig. 2 (c) requires significantly more initial charge of about 2.14 GWh. The presented results correspond to solutions located on the Pareto fronts, which balances economic cost and environmental impact. Along these fronts, the economically optimal solution relies heavily on battery storage and implements very limited hydrogen storage capacity for all of the three horizons. As the solutions shift toward the environmentally optimal region of the Pareto fronts, the amount of energy stored in hydrogen gradually increases and eventually exceeds that stored in batteries.

Figures 3 (a) and (b) zoom into two periods during these simulated time horizons where large discharges of the HES occurred in the models. It can be seen that hydrogen is used

TABLE III
TECHNICAL AND ECONOMIC PARAMETERS OF STORAGE TECHNOLOGIES FOR 2050

Technology	Parameter	Value	Unit	Source
Battery	CAPEX	270	k€/MWh	[32]
	O&M variable	1.7	€/MWh	[32]
	O&M fixed	570	€/MWh/year	[32]
	Lifetime	30	years	[32]
	Self-discharge	0.1	%/year	[32]
	Charge efficiency	0.985	-	[32]
	Discharge efficiency	0.975	-	[32]
Fuel Cell	CAPEX	40	k€/MW	[33]
	Efficiency	0.65	-	[33]
	Lifetime	10	years	[34]
Electrolyzer	CAPEX	410	k€/MW	[33]
	O&M variable	184	€/MWh	[35]
	O&M fixed	2	% CAPEX	[33]
	Consumption	50	kWh/kgH_2	[35]
	Lifetime	15	years	[35]
H_2 Tank	CAPEX	22	k€/MWh	[32]
	O&M fixed	3	% CAPEX	[36]
	Lifetime	30	years	[32]

TABLE IV
GWP OF STORAGE TECHNOLOGIES WITHOUT TRANSPORT FOR 2050

Technology	GWP	Unit	Source
Battery	127.45	kgCO_2eq/kWh	[37]
Fuel cell	29.47	kgCO_2eq/kW	[38]
Electrolyzer	244.58	kgCO_2eq/kW	[39]
H_2 Tank	8.49	kgCO_2eq/kWh	[38]

TABLE V
GWP TRANSPORT PHASE DATA FOR THE TECHNOLOGIES CONSIDERED FOR 2050

Technology	GWP transport phase
Battery	0.988 kgCO_2 eq/kWh
Fuel Cell	0.269 kgCO_2 eq/kW
Electrolyzer	0.537 kgCO_2 eq/kW
H_2 Tank	0.107 kgCO_2 eq/kWh

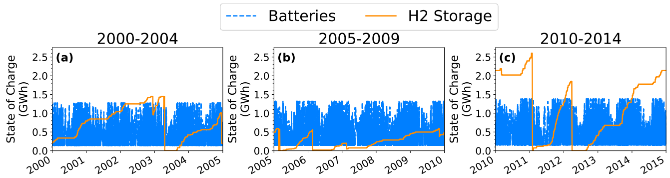

Fig. 2. Optimized storage operation from 2000 through 2004 (a), 2005 through 2009 (b), and 2010 through 2014 (c)

especially when there is a sharp drop in PV production for two or more consecutive days. For example, for the time period shown in Fig. 3 (a), the island went through a period of heavy rainfall that reduced PV production for two days by 38% as compared to the five-year daily median and mean. This led to a discharge of the HES of about 0.6 GWh.

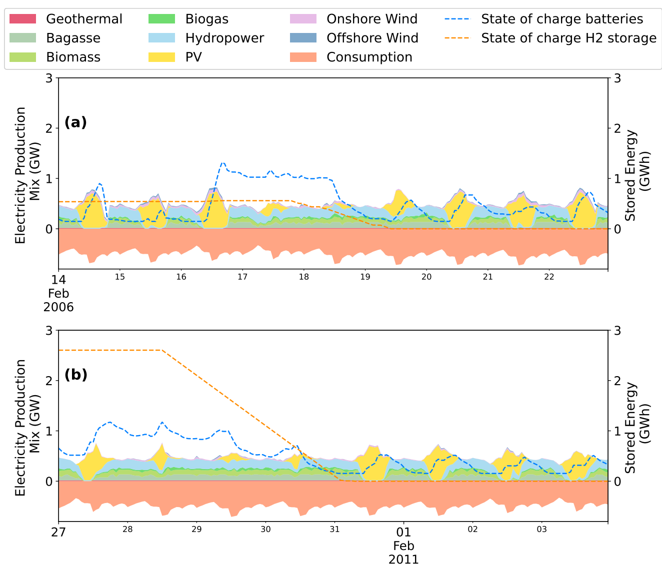

Fig. 3. Electricity generation, consumption, and storage state of charge for the 14th through the 22nd of February, 2006 (a) and the 27th of January through the 3rd of February, 2011 (b)

The largest discharge of hydrogen of all the five-year periods, 2.6 GWh, is shown in detail in Fig. 3 (b). Although the daily reduction in PV production was less than that shown in Fig. 3 (a) (approximately 75% of the daily five-year median and mean), the period lasted for three consecutive days rather than two and ultimately led to the need for a total combined HES size of 78.1 tonnes (2.6 GWh). Comparing the Fig. 2 sub-figures shows that the choice of the five-year weather time horizon has a significant impact on the optimal HES capacity. The time horizon of 2010 through 2014 implemented about a 340% more total HES capacity as compared to that implemented for 2000 through 2004. This is especially key given future climate uncertainty, especially since the cyclone frequency and intensity are expected to increase on the island due to climate change [40]. It is worth noting that across all three weather periods, the optimization did not select any transmission line capacity expansions. This holds despite the fact that several lines, were utilized up to their maximum capacity during some time periods, indicating congestion in the optimized network. These results suggest that, under the line expansion cost parameters, reinforcing the transmission network was more expensive than deploying storage solutions.

For stakeholders on Reunion island, these results suggest that while HES is infrequently used, it serves a critical role during multi-day PV shortfalls, preventing prolonged outages on the island. Considering the wide variation in optimal HES capacity between weather periods, capacity investment decisions must balance the risk of low PV production periods with increasing climate uncertainty and the inclusion of resilience margins with overall economic costs and apparent overcapacity. To compensate for the low annual utilization rate, it may be required to explicitly value the avoided curtailment, reliability benefits, and reduced dependence on imported fuels economically.

V. Conclusion

This work presented a methodology for optimizing long-duration HES implementation and dispatch on fully renewable islands, applied to Reunion Island over three five-year weather periods. Results showed that HES, unlike batteries, was used intermittently, reserved for poor PV production periods lasting two or more days. The differing HES capacities across the three periods underscore the influence of weather-period selection, highlighting the need to account for future weather uncertainty to ensure adequate HES implementation and dispatch. Furthermore, all three time horizon results show limited use of the HES, which may not be favorable from a technical perspective, as long periods of inactivity for fuel cells can lead to degradation of fuel cell components, affecting performance and durability [41]. This aspect was not modeled and warrants further investigation and comparison to other forms of long-duration energy storage technologies or demand management strategies.

Finally, since the capacity expansion and dispatch optimization model took all five years of the time horizon into consideration, also known as a full-foresight model, multi-year charging behavior can be seen, given that the model knows a significant poor weather event is going to happen in the future. For example, 2 (a) shows the HES being charged for over three years before a discharge in 2003. In reality, however, such long-duration weather forecasting is highly uncertain and practically infeasible beyond a few days to two weeks [42]. As a result, this type of foresight-driven behavior may not reflect realistic operational planning and underestimate long-duration energy storage needs. Future work will focus on implementing a more realistic approach to capture the inherent uncertainty of future weather and system conditions and realistic forecast prediction timescales via the rolling-horizon framework or stochastic methods.

Acknowledgment

This work has been supported by the EIPHI Graduate School (contract ANR-17-EURE-0002), the Region Bourgogne Franche-Comté and the HyLES project (contract ANR-20-CE05-0035).

References

[1] IRENA, *Transforming Small-Island Power Systems: Technical Planning Studies for the Integration of Variable Renewables.* Abu Dhabi: International Renewable Energy Agency, 2018.

[2] J. M. Lassalle, D. F. Martínez, and L. V. Fernández, "Optimisation of hybrid renewable energy systems on islands: A review," *Island Studies Journal*, vol. 17, no. 1, pp. 221–242, 2022.

[3] O. Bamisile, D. Cai, H. Adun, M. Dagbasi, C. C. Ukwuoma, Q. Huang, N. Johnson, and O. Bamisile, "Towards renewables development: Review of optimization techniques for energy storage and hybrid renewable energy systems," *Heliyon*, vol. 10, no. 19, 2024.

[4] F. Nadeem, S. M. S. Hussain, P. K. Tiwari, A. K. Goswami, and T. S. Ustun, "Comparative review of energy storage systems, their roles, and impacts on future power systems," *IEEE Access*, vol. 7, pp. 4555–4585, 2019.

[5] R. Khakimov, A. Moskvin, and O. Zhdaneev, "Hydrogen as a key technology for long-term & seasonal energy storage applications," pp. 374–381, 2024.

[6] C. G. Meza, C. Z. Rodríguez, C. A. D'Aquino, N. B. Amado, A. Rodrigues, and I. L. Sauer, "Toward a 100% renewable island: A case study of ometepe's energy mix," *Renewable Energy*, vol. 132, pp. 628–648, 2019.

[7] B. Guinot, B. Champel, F. Montignac, E. Lemaire, D. Vannucci, S. Sailler, and Y. Bultel, "Techno-economic study of a PV-hydrogen-battery hybrid system for off-grid power supply: Impact of performances' ageing on optimal system sizing and competitiveness," *International Journal of Hydrogen Energy*, vol. 40, no. 1, pp. 623–632, Jan. 2015.

[8] D. Ipsakis, S. Voutetakis, P. Seferlis, F. Stergiopoulos, S. Papadopoulou, and C. Elmasides, "The effect of the hysteresis band on power management strategies in a stand-alone power system," *Energy*, vol. 33, no. 10, pp. 1537–1550, Oct. 2008.

[9] D. Hernández-Torres, C. Turpin, X. Roboam, and B. Sareni, "Techno-economical optimization of wind power production including lithium and/or hydrogen sizing in the context of the day ahead market in island grids," *Mathematics and Computers in Simulation*, vol. 158, pp. 162–178, Apr. 2019.

[10] A. Escamilla, D. Sánchez, and L. García-Rodríguez, "Techno-economic study of Power-to-Power renewable energy storage based on the smart integration of battery, hydrogen, and micro gas turbine technologies," *Energy Conversion and Management: X*, vol. 18, p. 100368, Apr. 2023.

[11] I. Petkov and P. Gabrielli, "Power-to-hydrogen as seasonal energy storage: An uncertainty analysis for optimal design of low-carbon multi-energy systems," *Applied Energy*, vol. 274, p. 115197, Sep. 2020.

[12] Commission de régulation de l'énergie (CRE), "Transition énergétique dans les ZNI," https://www.cre.fr/electricite/transition-energetique-dans-les-zni.html, 2025, consulté le 22 juillet 2025.

[13] A. François, "Modélisation et optimisation de réseaux électriques insulaires à moyen et long terme : étude de l'impact de l'intégration de l'hydrogène à la réunion – application aux mobilités et au stockage réseau," Ph.D. dissertation, Université Bourgogne Franche-Comté, oct 2024, accessed 2025-03-20.

[14] H. C. Hesse, M. Schimpe, D. Kucevic, and A. Jossen, "Lithium-Ion Battery Storage for the Grid—A Review of Stationary Battery Storage System Design Tailored for Applications in Modern Power Grids," *Energies*, vol. 10, no. 12, p. 2107, Dec. 2017.

[15] T. Brown, J. Hörsch, and D. Schlachtberger, "PyPSA: Python for Power System Analysis," *Journal of Open Research Software*, vol. 6, no. 1, p. 4, Jan. 2018.

[16] G. K. Karayel, N. Javani, and I. Dincer, "A comprehensive assessment of energy storage options for green hydrogen," *Energy Conversion and Management*, 2023.

[17] H. Montazerinejad and U. Eicker, "Recent development of heat and power generation using renewable fuels: A comprehensive review," *Renewable and Sustainable Energy Reviews*, 2022.

[18] H. Chen, T. N. Cong, W. Yang, C. Tan, Y. Li, and Y. Ding, "Progress in electrical energy storage system: A critical review," *Prog. Nat. Sci.*, vol. 19, no. 3, pp. 291–312, Mar. 2009.

[19] G. Mantegna, W. Ricks, A. Manocha, N. Patankar, D. Mallapragada, and J. Jenkins, "Establishing best practices for modeling long duration energy storage in deeply decarbonized energy systems," 2024. [Online]. Available: https://arxiv.org/abs/2404.17474

[20] P. A. Sánchez-Pérez, M. Staadecker, J. Szinai, S. Kurtz, and P. Hidalgo-Gonzalez, "Effect of modeled time horizon on quantifying the need for long-duration storage," *Applied Energy*, vol. 317, p. 119022, 2022.

[21] O. Ruhnau and S. Qvist, "Storage requirements in a 100% renewable electricity system: extreme events and inter-annual variability," *Environmental Research Letters*, vol. 17, no. 4, p. 044018, 2022.

[22] D. Chotard, T. Lefillatre, N. Mairet, F. Babonneau, and A. Haurie, "Vers l'autonomie énergétique des Zones non Interconnectées (ZNI)," ADEME, Tech. Rep., 2018.

[23] INSEE, "La réunion (974) – key figures," 2025, accessed: 2025-07-23. [Online]. Available: https://www.insee.fr/en/statistiques/6457611?geo=DEP-974

[24] E. Lagabrielle, M. Rouget, T. Le Bourgeois, K. Payet, L. Durieux, S. Baret, J. Dupont, and D. Strasberg, "Integrating conservation, restoration and land-use planning in islands—an illustrative case study in réunion island (western indian ocean)," *Landscape and Urban Planning*, vol. 101, no. 2, pp. 120–130, 2011.

[25] Observatoire Énergie Réunion, "Bilan Énergétique de la réunion – chiffres clés 2023," PDF brochure, Sep. 2024, Édition 2024; accessed via OER website; Accessed: 2025-07-23. [Online]. Available: https://oer.energies-reunion.com/sites/observatoire-energie-reunion/files/202409/PLAQUETTE\%20CHIFFRES\%20CLES_2024_FR_WEB_0.pdf

[26] F. Babonneau, S. Biscaglia, D. Chotard, A. Haurie, N. Mairet, and T. Lefillatre, "Assessing a transition to 100% renewable power generation in a non-interconnected area: a case study for la réunion island," *Environmental Modeling & Assessment*, vol. 26, no. 6, pp. 911–926, 2021.

[27] A. François, R. Roche, D. Grondin, and M. Benne, "Assessment of medium and long term scenarios for the electrical autonomy in island territories: The Reunion Island case study," *Renewable Energy*, vol. 216, p. 119093, Nov. 2023.

[28] EDF, "Open Data EDF Réunion," https://opendata-reunion.edf.fr/pages/home0/.

[29] ADEME, "Prospective - Transitions 2050," Tech. Rep., 2021.

[30] S. His and G. Dubois, "La transition énergétique dans les zones non-interconnectées de France : l'impasse de l'usage massif de la biomasse importée," Energies renouvelables pour tous, Tech. Rep., 2024.

[31] Ministère de la Transition écologique et solidaire, "Information GES des prestations de transport : Guide méthodologique," Ministère de la Transition écologique et solidaire, France, Rapport technique, 2018.

[32] Danish Energy Agency, "Technology Data for Energy Storage," 2017.

[33] F. Zenith, R. Isaac, A. Hoffrichter, M. S. Thomassen, and S. Møller-Holst, "Techno-economic analysis of freight railway electrification by overhead line, hydrogen and batteries: Case studies in Norway and USA," *Proceedings of the Institution of Mechanical Engineers, Part F: Journal of Rail and Rapid Transit*, vol. 234, no. 7, pp. 791–802, Aug. 2020.

[34] Danish Energy Agency, "Technology Data for Generation of Electricity and District Heating," 2024.

[35] D. Wickham, A. Hawkes, and F. Jalil-Vega, "Hydrogen supply chain optimisation for the transport sector – Focus on hydrogen purity and purification requirements," *Applied Energy*, vol. 305, p. 117740, Jan. 2022.

[36] H. Kim, N. Hartmann, M. Zeller, R. Luise, and T. Soylu, "Comparative TCO Analysis of Battery Electric and Hydrogen Fuel Cell Buses for Public Transport System in Small to Midsize Cities," *Energies*, vol. 14, no. 14, p. 4384, Jan. 2021.

[37] C. Robert, A. Ravey, R. Perey, and D. Hissel, "Environmental impacts of batteries for transportation application according to different life cycle steps," in *2022 IEEE Vehicle Power and Propulsion Conference (VPPC)*, Nov. 2022, pp. 1–6.

[38] ——, "Potentiel de Réchauffement Global et impacts sociétaux d'un système Pile à Hydrogène," in *3éme Réunion Plénières de La Fédération Hydrogène (FRH2) Du CNRS*, Saint-Gilles, France, May 2023.

[39] A. Lotrič, M. Sekavčnik, I. Kuštrin, and M. Mori, "Life-cycle assessment of hydrogen technologies with the focus on EU critical raw materials and end-of-life strategies," *International Journal of Hydrogen Energy*, vol. 46, no. 16, pp. 10 143–10 160, Mar. 2021.

[40] M.-D. Leroux, F. Bonnardot, S. Somot, A. Alias, S. Kotomangazafy, A.-O. S. Ridhoine, P. Veerabadren, and V. Amélie, "Developing climate services for vulnerable islands in the southwest indian ocean: A combined statistical and dynamical cmip6 downscaling approach for climate change assessment," *Climate Services*, vol. 34, p. 100491, 2024.

[41] W. Schmittinger and A. Vahidi, "A review of the main parameters influencing long-term performance and durability of PEM fuel cells," *Journal of Power Sources*, vol. 180, no. 1, pp. 1–14, May 2008.

[42] B.-W. Shen, R. A. Pielke Sr, X. Zeng, and X. Zeng, "Exploring the origin of the two-week predictability limit: A revisit of lorenz's predictability studies in the 1960s," *Atmosphere*, vol. 15, no. 7, p. 837, 2024.